Adhesion in the life history of the Australian Sea Urchin,

Holopneustes purpurascens

David M. Connolly

Masters of Research

Faculty of Science and Engineering, Department of Biological Sciences, Macquarie University, NSW, 2109

Supervisor: A/Prof. Jane Williamson

Formatted for *Marine Ecology Progress Series*

Submission Date:

9/11/15

Word Count:

7079

Declaration

The methods and results listed below was the work of Thomas Desvignes from September 2006 to February 2007 under the supervision of Jane Williamson.

Method: Tube feet and test analysis, morphology and ultrastructure of the tube foot disc

Results: External morphology of the tube feet, tube feet histology

Supplementary Material: Figure S2 and Figure S3

All other research outlined in this report is of my own work.

Signature

D Connolly

Name

David Connolly

Date

5/11/15

Abstract

The Australian sea urchin *Holopneustes purpurascens* undergoes a substantial increase in body size before risking the transition from its initial host alga *Delisea pulchra* to the much preferred kelp, *Ecklonia radiata*. It is thought that smaller urchins lack the adhesive strength of larger urchins and are unable to enmesh themselves in the fronds of the more rigid *E. radiata,* and therefore must settle in the softer *D. pulchra.* Using a number of key morphological and adhesive traits we aimed to determine the role of temporary gel adhesion in this shift. While larger urchins had more tube feet, a larger disc surface area and a greater adhesive coverage, there was no significant difference in the detachment force required between large, medium and small urchins on both host plants. Detachment force was significantly less for urchins on *D. pulchra* than those on *E. radiata* and is a finding suggested for further research. Laminar flow flume testing indicated that the smallest urchins adhered better under high flow rates, declining as size increased. Overall we concluded that adhesion is a substantial contributor to the ontogenetic shift of *H. purpurascens* in conjunction with one or more alternate mechanisms.

Key Words: *Delisea pulchra, Ecklonia radiata,* temporary gel-adhesion, ontogenetic shift

Introduction

Body size remains one of the most important features of an organism, influencing predation risk, vulnerability to environmental pressures and resource use (Werner & Gilliam 1984). Ontogenetic shifts outline changes in resource use as body size increases from birth or metamorphosis to maximum size; this may include the use of multiple habitat types and diet change (Werner & Gilliam 1984). Examples of these shifts can be seen in the transition of a range of organisms from complex to open habitat, shallow to deep water environments or the increase in prey size or type as body size increases (Hereu et al. 2005, Graham et al. 2007, Vincent et al. 2007). These size specific interactions are vitally important in shaping life history, species interaction and community demographics (Werner & Gilliam 1984). In contrast to basic niche shifts, which can vary depending on their function - seasonal spawning or diel feeding - ontogenetic shifts present a far more permanent shift in resource use (Kimirei et al. 2013). The associated benefits of undertaking an ontogenetic shift therefore must far outweigh the risks and effects of the transition for the shift to occur (Dahlgren & Eggleston 2000). Understanding these mechanisms that drive and facilitate these shifts is fundamentally important to our understanding of ecosystem interactions (Werner & Gilliam 1984). Ontogenetic shifts in marine systems are both extremely common and taxonomically diverse, but the drivers of these shifts are often poorly understood. One known ontogenetic shift has been documented in the Australian sea urchin *Holopneustes purpurascens* (Temnopleuridae: Echinodermata).

Holopneustes purpurascens occurs along Australia's east coast living and grazing amongst sublittoral kelp beds (Steinberg 1995). *Holopneustes purpurascens* abides by a less conventional sea urchin lifestyle, and instead of living and feeding directly off the substrate as most urchins do, *H. purpurascens* is found inhabiting the fronds of both the red alga *Delisea pulchra* and the brown kelp *Ecklonia radiata* (Steinberg 1995, Williamson et al. 2004). By living in the algal canopy above the substrata, *H. purpurascens* creates a shelter from predators and environmental pressures, such as wave action (Bell et al. 2014). The presence of *H. purpurascens* on host plants, *D. pulchra* and *E. radiata* produces a distinctive size driven bimodal distribution (Williamson et al. 2004). Individuals on the host kelp *E. radiata* are

significantly larger than those found on *D. pulchra*, whilst no new recruits (i.e. extremely small individuals) occur on *E. radiata* (Williamson et al. 2004). New recruits settle on *D. pulchra* in response to the release of the chemical histamine by the alga; histamine is not found in *E. radiata* (Swanson et al. 2006). Following substantial growth in body size, *H. purpurascens* then undergoes a stringent ontogenetic shift from *D. pulchra* to *E. radiata* (Williamson et al. 2004). The presence of halogenated furanones in *D. pulchra,* which deters feeding and reduces survival, growth and reproduction of *H. purpurascens*, may indicate the benefits of transitioning to *E. radiata* as a long term host, despite the risks associated with transition (Williamson et al. 2004). To transition from one host to the next, *H. purpurascens* must undergo substantial risk in the form of increased predation and dislodgment by wave action. This poses the question of what is preventing *H. purpurascens* from directly settling onto the 'much preferred' *E. radiata* over *D. pulchra*. It is suggested that this behaviour may be a result of a lack of adhesive strength, and that smaller urchins may be unable to enmesh themselves in the fronds of the more rigid *E. radiata,* whilst less adhesive strength is required to wrap themselves in the more flexible and foliose *D. pulchra.* (Williamson et al. 2004).

Adhesive strength is a product of a unique mechanism of surface attachment known as temporary gel-adhesion. Sea urchins such as *H. purpurascens* often occupy near shore regions that can be some of the most stressful environments to inhabit, and as a result their survival hinges on the organism's innate ability to cope with such hydrodynamic energy (Denny et al. 1985). These organisms attach to the surface via small, extensible stems, bearing flattened discs known as tube feet or podia (Flammang 1996). Tube feet contain a dual-gland system, consisting of two distinct non ciliated cell types, responsible for the secretion of a gel-like adhesive and de-adhesive (Flammang 1996). A thin film of adhesive is secreted via the podial disc cuticle that bonds the tube feet to a particular surface, whilst the de-adhesive works by removing the outermost layer of the cuticle, initiating detachment. The remaining layer on the surface is commonly referred to as the footprint (Flammang 1996). Temporary adhesion by urchins is of considerable interest due to its unique properties: podia have a high adhesive strength for their size, measuring from 0.09 to 0.54MPa, whilst structurally, remaining quite soft at 8.1 kPa (Santos et al. 2005; Santos & Flammang 2008). In comparison, adhesive strength

in other non-permanent marine invertebrates measures between 0.1 and 0.5 MPa (Smith 2006).

This research examined the role of temporary gel-adhesion in the ontogenetic shift of *H. purpurascens* from *D. pulchra* to *E. radiata* by examining a number of key morphological and adhesive traits. Firstly the number of tube feet on *H. purpurascens* in relation to its size was examined, where it is expected that larger urchins are composed of a greater number of tube feet. Secondly, the attachment qualities amongst sizes were examined, with the prediction that footprint surface area and quality will differ amongst size classes. Thirdly, the detachment force required to remove *H. purpurascens* from both its host algae were assessed based on the prediction that larger sizes of individuals will require a greater detachment force than smaller sized urchins on the kelp, *E. radiata*; whilst on *D. pulchra* larger urchins would detach more easily than smaller ones. Finally, adhesion under laminar flow was assessed to establish a maximum flow rate at which different sizes of *H. purpurascens* could attach to *E. radiata* as well as to establish flow rates at which *H. purpurascens* can adhere to for prolonged exposure. It was predicted that as urchin size increased the maximum flow rate needed to induce detachment would also increase. Furthermore, as a novel study of adhesion in *H. purpurascens,* the function and structure of the tube feet as a means of temporary gel adhesion was assessed via microscopic techniques including, light microscopy and scanning electron microscopy.

Method

The sea urchin *Holopneustes purpurascens*, the kelp *Ecklonia radiata* and the red alga *Delisea pulchra* were collected from sublittoral areas up to 5m depth in the following locations around Sydney: Fairlight (33°48'1"S, 151°16'3"E), Bare Island (33°59'29.0"S, 151°13'51.4"E) Balmoral (33°49'22.6"S, 151°15'08.5"E) and Long Bay (33°57'55.7"S, 151°15'19.5"E). Collections were done on snorkel with *H. purpurascens, E. radiata* and *D. pulchra* transported to the seawater facility at Macquarie University. Urchins were held in filtered (20/50/100µm) and UV sterilised recirculating seawater (FSW) tanks throughout the experiment under the following conditions: Temperature 21.0±3^{0}C, pH 8.0±0.1, Salinity 36.0±1.0ppt, 12:12 light dark cycle, ~1L/min. Following the completion of the experiment urchins were released at the location of their collection.

Holopneustes purpurascens were grouped for experiments according to maximum test diameter (excluding spines) in the following size classes: Small (0-30mm), Medium (31-45mm) and Large (>45mm) (Williamson et al. 2004). Size classes were created according to host algal use: small individuals are primarily found on *D. pulchra*, medium, found on both *D. pulchra* and *E. radiata* – the transitioning period – and large individuals found solely on *E. radiata* (Williamson et al. 2004).

Fertilization:

To gain sizes of *Holopneustes purpurascens* under <1mm, reproductively mature urchins were injected through the peristomial membrane with 1-2ml of 0.5M KCl and agitated by slow shaking. Urchins were then placed oral side up in a beaker and monitored for signs of gamete emission. Sperm were collected dry, via pipette off the urchins' test, whilst eggs were released into FSW. Following spawning, all eggs and sperm were mixed for a period of 15mins and then the eggs were removed from the gamete mixture to prevent polyspermy, and placed into a beaker of FSW. The beaker was covered with parafilm, and air slowly bubbled into beaker to prevent stagnation. Water was filtered through a 60µm mesh using a venturi pump and water

replaced daily. Newly metamorphosed individuals were used to calculate the number of tube feet in urchins <1mm in size.

Tube feet footprints

To examine tube feet adhesion amongst different locations on the test, footprints were used as a proxy for adhesion. *H. purpurascens* were submerged in an aerated container of FSW, where a microscope slide was presented to the tube feet on the oral side of the urchin. Once tube feet were firmly attached, the slide was removed in the direction of natural extension and immediately immersed in 0.05% aqueous solution of the crystal violet dye (as per Santos & Flammang 2006) for 2 minutes to stain the footprints that remained following tube foot detachment. Following staining each microscope slide was then dipped consecutively into two jars of filtered water to remove any excess crystal violet stain. The process was repeated for the tube feet at the ambitus of *H. purpurascens'* test and then again for those on the aboral side, for a total of 3 slides per individual.

Footprints were viewed under a BX53 light microscope at 10x magnification. From each slide, 20 footprints were digitally imaged using cellSENS v.1.6 and categorised as either 'full attachment' or 'partial attachment' (Figure 3A, 3B). Partial attachment was defined as the "loss" of one third or greater of the footprints' stained area. Urchins <1mm in size were also examined for footprints, but no footprints were observable following staining. Footprints amongst locations and size classes were analysed via nested Analysis of Variance (ANOVA).

Footprint Size

To determine the maximum area of the podial disc available for adhesion, the size of the footprints were assessed. Footprints were randomly chosen from the oral, ambitus and aboral sides of each urchin, for a total of 10 footprints per urchin. Surface area was calculated using ImageJ v.1.49 software using an ellipsis of best fit around the footprint; if an appropriate ellipsis could not be formed using the footprint it was removed and another chosen from the same location on the urchin. Footprint surface area between individuals within size classes was compared via a nested ANOVA (Size Class x Diameter x Tube foot surface area).

Adhesion amongst size classes

To determine the strength of attachment of individuals to fronds of *E. radiata* and *D. pulchra*, an INSTRON mechanical testing machine (INSTRON 5542) was used. Fronds of algae were trimmed and clamped to the bottom of a large beaker filled with fresh seawater (see Supplementary Figure S1). The beaker was placed on the INSTRON directly under the machine's tensile arm. Individual *H. purpurascens* were placed in a sparsely meshed Wilson's catch net that was then attached to the tensile arm. Before each trial, each urchin was gently held down onto the clamped algae for 10 seconds to allow it to attach. The INSTRON was set to apply an upward lift at a rate of 15mm/min and to record force continuously until the point of urchin detachment from the alga. Following a trial, the number of tube feet ruptured by detachment was counted. Each individual was tested oral and aboral side down. If attachment was inadequate or the alga moved during the trial, the test was aborted.

Data on detachment forces for the oral and aboral testing of *H. purpurascens* on *D. pulchra* was log transformed to achieve normality before comparing it with a one way ANOVA (Detachment force). Data on detachment forces for *E. radiata* did not require transformation. To examine the influence of size on detachment force amongst host species, *H. purpurascens* was divided into size classes and mean detachment force was analysed using a two factor ANOVA (both factors fixed - Mean detachment force x Size class) on both oral and aboral sides. Data was then analysed post hoc via Tukey test.

During the detachment force testing conducted on the INSTRON machine, the number of tube feet ruptured at detachment was also counted. Statistical analysis was conducted using a Welch ANOVA (Tube feet loss x Size class) after failing homogeneity of variances, whilst the Games-Howell post hoc test was employed to discern differences between size classes.

Adhesion against laminar flow

To test attachment strength of *H. purpurascens* against tidal flow, urchins were first transported to the Sydney Institute of Marine Science (SIMS) and kept in filtered (100µm) flow through tanks. Seawater was taken directly from an inlet pipe from Chowder Bay, Sydney

Harbour and held under the following conditions: Temperature ~21^{0}C, pH 8.05±0.05, Salinity ~35ppt, 12:12 light dark cycle, ~1.5L/min. Two tests using a high-speed circulating seawater flume tank were done on *H. purpurascens* under laminar flow: a maximum flow test and a prolonged exposure test. The first test determined the maximum laminar flow reached before individuals detached from a frond of *E. radiata.* The frond was clamped and suspended at the centre of the tank. Before each trial, the urchin was given time to enshroud themselves in the frond. Flow was then initiated and increased continuously (0.25m s^{-2}) until detachment occurred and the maximum flow recorded. The second test determined tenacity during prolonged exposure to constant flow rates. Urchins were subjected to each flow rate for 1 minute until they reached their maximum exposure flow before detachment. Each test began with no flow and was accelerated at 0.25m s^{-2} until the desired flow rate was achieved. If an urchin was unable to sustain adhesion during the 1 minute test time, the previous flow rate at which it could complete was declared the prolonged exposure score. Each urchin's specific flow rates were examined randomly, with the same urchin never tested twice in a row.

Urchin size classes tested in maximum speed and prolonged exposure tests were analysed using a two factor ANOVA (Detachment speed x Size class). A post hoc Tukey test was then implemented to differentiate between size classes on the maximum speed test. Maximum detachment speed was also measured against surface area in a linear regression (Detachment speed x Surface area) . Surface area [SA] was calculated using 2 measurements - 2 diameter [D], oral-aboral height [H] - and the formula for projected surface area:

$$SA = \frac{(D\ x\ H\ x\ \pi)}{4}$$

Tube feet and test analysis

To examine the relationship between the number of tube feet and test morphology, urchins were euthanised, cleaned and immersed in 2.5% Sodium Hypochlorite for 2 hours. The number of tube feet was counted using the rows of pores located on each of the urchins' ambulacrum - two pores indicate a single tube foot. Digital images of the test used in counting were taken with a QImaging camera set up on an Olympus SZX9 microscope. Urchin test morphology

(diameter and volume) was also examined using Vernier callipers measured to the nearest 0.05mm. Volume was calculated using formula for the volume of an ellipsoid. Urchins under 1mm in size were examined under an Olympus BX51 light microscope and imaged using a Sumix-160x camera mounted onto the microscope. Tube feet were counted and urchin diameter was measured using Image J v.1.49. The relationship between test diameter and the number of tube feet on *H. purpurascens* was examined using a linear regression (Diameter x Tube feet), whilst the relationship between volume and tube feet was measured with a quadratic equation (Volume x Tube feet).

Morphology and ultrastructure of tube foot disc

To examine the external morphology and internal structure, tube feet from three randomly selected urchins were dissected and examined under Light Microscopy (LM) and Scanning Electron Microscopy (SEM). For LM, tube feet were cut on the ambitus and immediately fixed in 3% glutaraldehyde in cacodylate buffer (0.1 M, pH 7.8) for 3h at 4°C. Tube feet were then rinsed in cacodylate buffer and post-fixed for 1h in 1% Osmium Tetroxide (OsO_4) in the same buffer. After a final buffer wash, half of the tube feet were decalcified with a solution of ascorbic acid 2% and 0.3M of NaCl in a 1:1 ratio for 3 hours (Dietrich & Fontaine 1975). Tube feet were serially dehydrated in Analytical Grade Ethanol in the following manner: 15 mins in 50%, then 2hours 15mins in each of 70%, 80%, 90%, 95% and 100% EtOH. Tube feet were then transferred in graded LR White Resin / Ethanol solutions according to a 1:3 ratio for 20 hours, 1:2 for 2 hours 20 minutes, 1:1, 2:1, 3:1 and 3 hours 20 minutes at 1:0 until finally embedded in LR White Resin. Longitudinal semi-thin sections (0.7µm in thickness) were cut with a Leica ultramicrotome equipped with glass knife and stained with Methylene blue and observed under a Olympus BX52 microscope. Slides were photographed by a Scion Corporation CFW-1310C camera set up on an Olympus BX50 binocular.

For SEM, tube feet were cut on each ambulacrum from three areas on the urchin: oral, ambitus and aboral. Some ambital, oral and aboral tube feet were also dissected immediately after attachment on a glass slide. The freshly cut tube feet were fixed for 24 hours in Non-Acetic Bouin's fluid, then left for 4 days in 70% Analytical Grade Ethanol and dehydrated for 2 hours 10

minutes at 80%, 90%, 95%, 100% and then 1 hour at 100%. They were then dried by the critical point method (using CO_2 as transmission fluid), mounted on aluminium stubs and coated with gold in a sputter coater (Flammang & et al. 1994; Santos & Flammang 2006).

Skeletal elements of the tube foot disc were obtained by incubating dissected discs in 5% Sodium Hypochlorite for 5 min. Cleaned ossicles and spicules were rinsed in distilled water, air-dried, mounted on aluminium stubs and coated with gold. Both tube feet and skeletal elements were observed with a Jeol JSM 6480LA scanning electron microscope.

Results

Number of tube feet and morphometrics

The number of tube feet increased linearly with test diameter (R^2=0.762, $F_{1,18}$=57.737, P<0.01) (Figure 1). Of the 19 urchins measuring under <1mm, tube feet numbers ranged from 5 to 12, whilst the mean diameter was 0.56mm. Quadratic regression also revealed a significant positive relationship between the number of tube feet and urchin volume (R^2=0.915, $F_{2,28}$=149.957, P<0.01). The number of tube feet increase rapidly until ~2000 tube feet were present, before plateauing at larger volumes (>40000mm^3) (Figure 2).

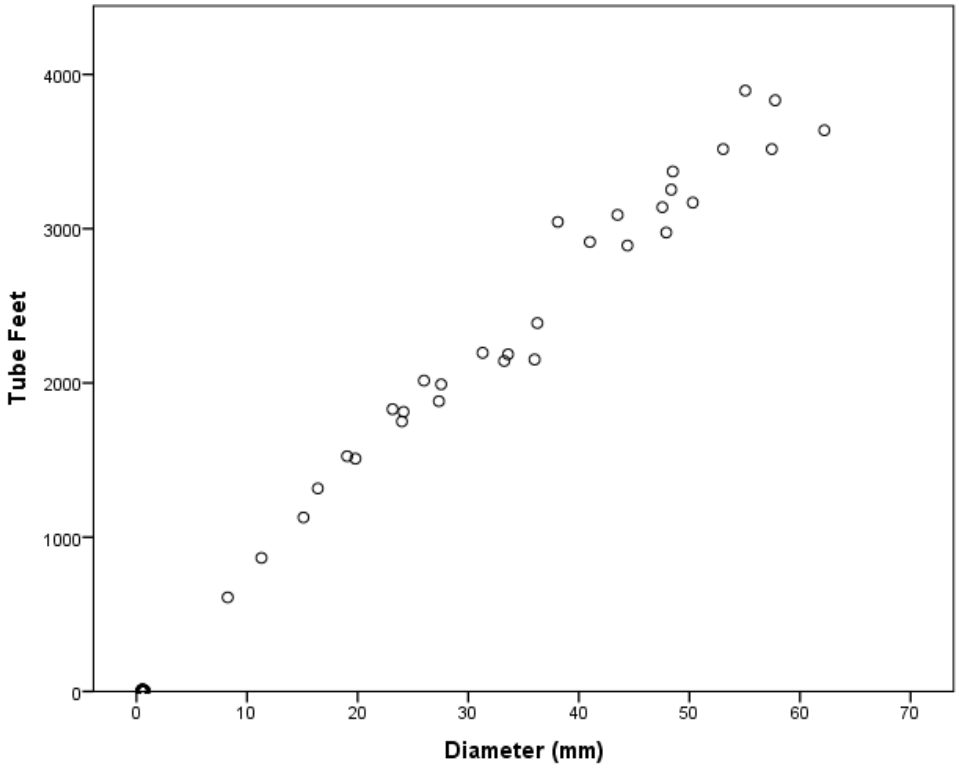

Figure 1: Relationship between urchin diameter and the number of tube feet for *Holopneustes purpurascens* (n=50). Equation: Diameter= -0.213 + 0.15(Tube Feet).

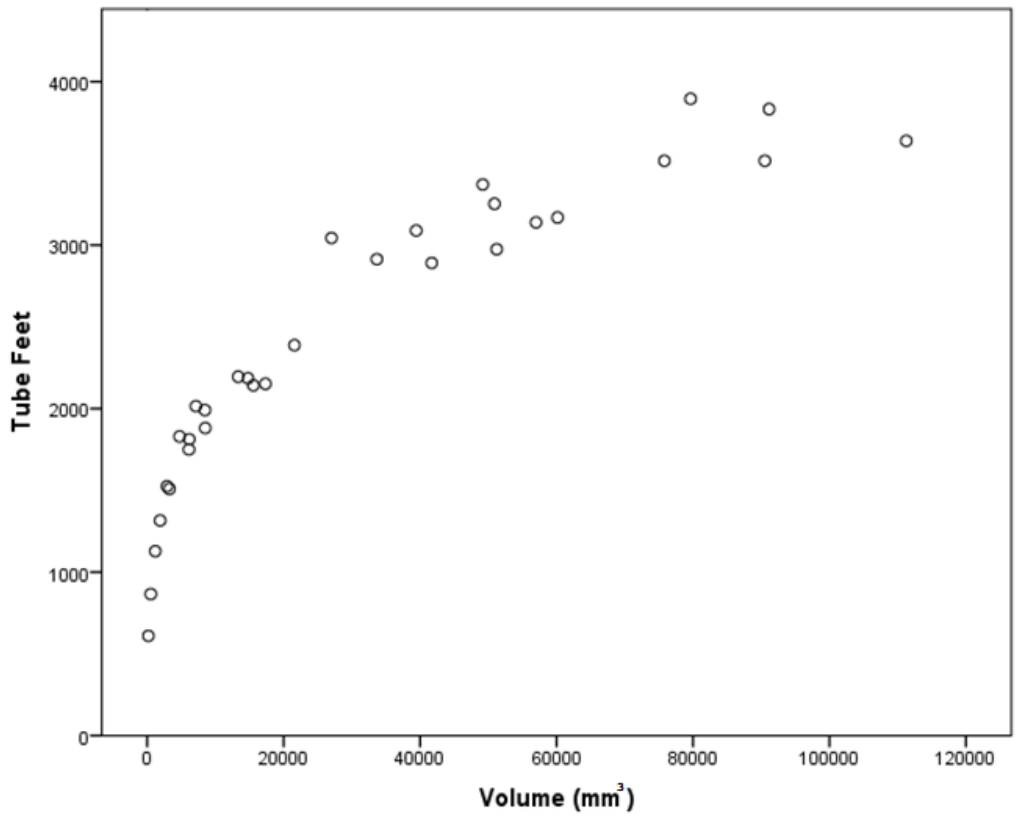

Figure 2: Quadratic regression between the number of tube feet and test volume for *Holopneustes purpurascens* (n=31). Equation: Tube Feet = 15621 -28.3469(Volume) + 0.13 $(Volume)^2$.

Tube feet footprints

Tube feet footprints were either circular or irregular in shape and with all cases there was little evidence of staining in the central circle of the footprint (Figure 3A, B). The area of tube feet attachment did not differ between the oral, ambitus and aboral areas (Nested ANOVA, $_{6,144}$=0.91, P=0.489). Whilst adhesion did differ between size classes (Nested ANOVA, $F_{2,144}$=35.1, P < 0.01). A subsequent post hoc Tukey test revealed that large urchins had significantly higher numbers of fully attached footprints (p<0.01), whilst there was no detectable difference between medium and small size classes (p=0.762) (Figure 4).

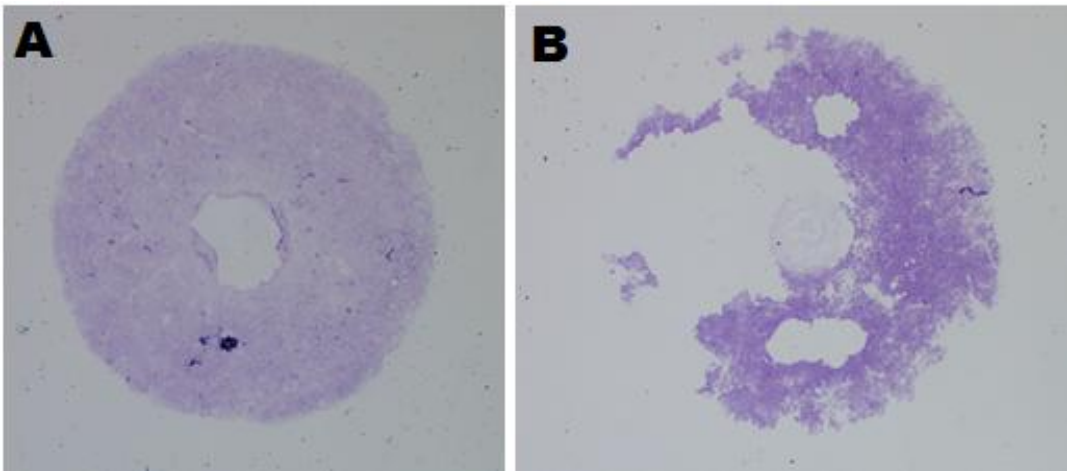

Figure 3: Footprints of *Holopneustes purpurascens* (**A**) Full Attachment (**B**) Partial Attachment.

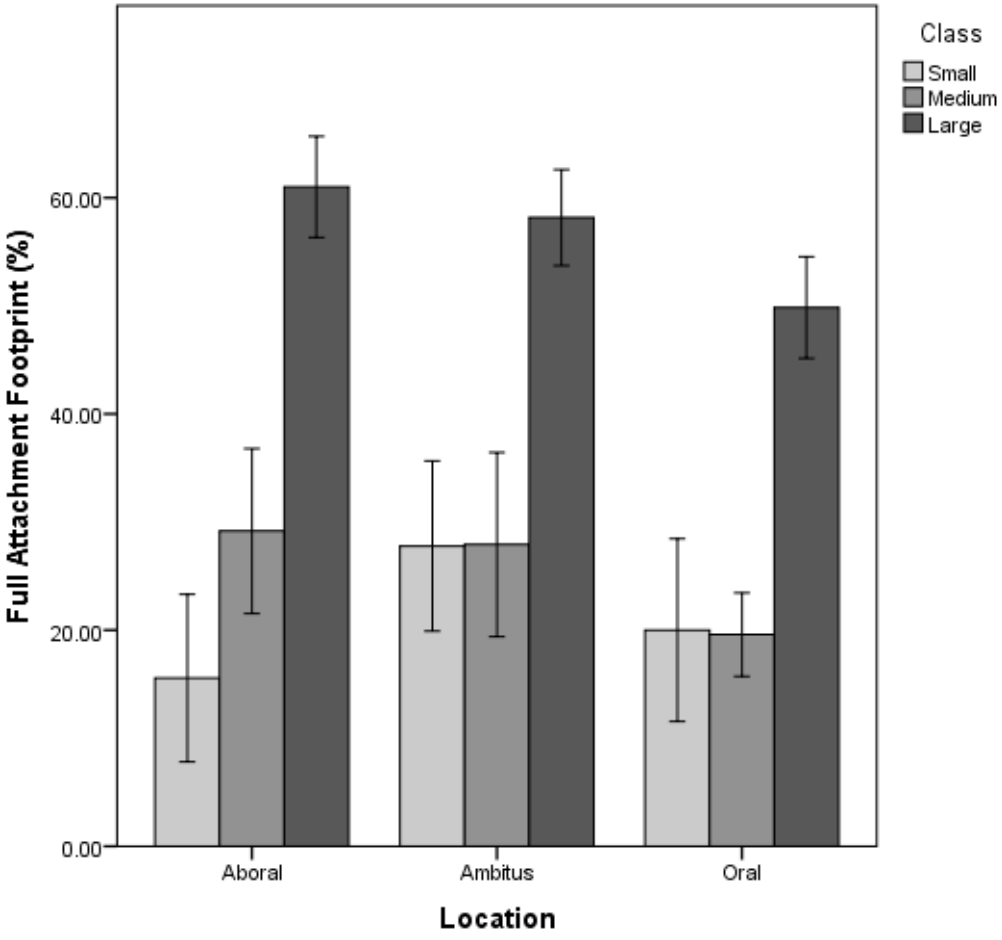

Figure 4: Percentage of ' fully attached' tube feet for the 3 locations on *Holopneustes purpurascens* (mean ±1SE; Aboral, Ambitus, Oral; n=51).

Footprint Size

Tube foot disc surface area increased with increasing urchin size. The larger the urchins, the larger the disc maximum (nested ANOVA, $F_{1,18}$=43.639, P<0.01) (Figure 5). Disc surface area ranged from 0.092 to 0.415mm^2. Medium and large sized urchin classes displayed a wider range of tube foot surface area than the small size class urchins.

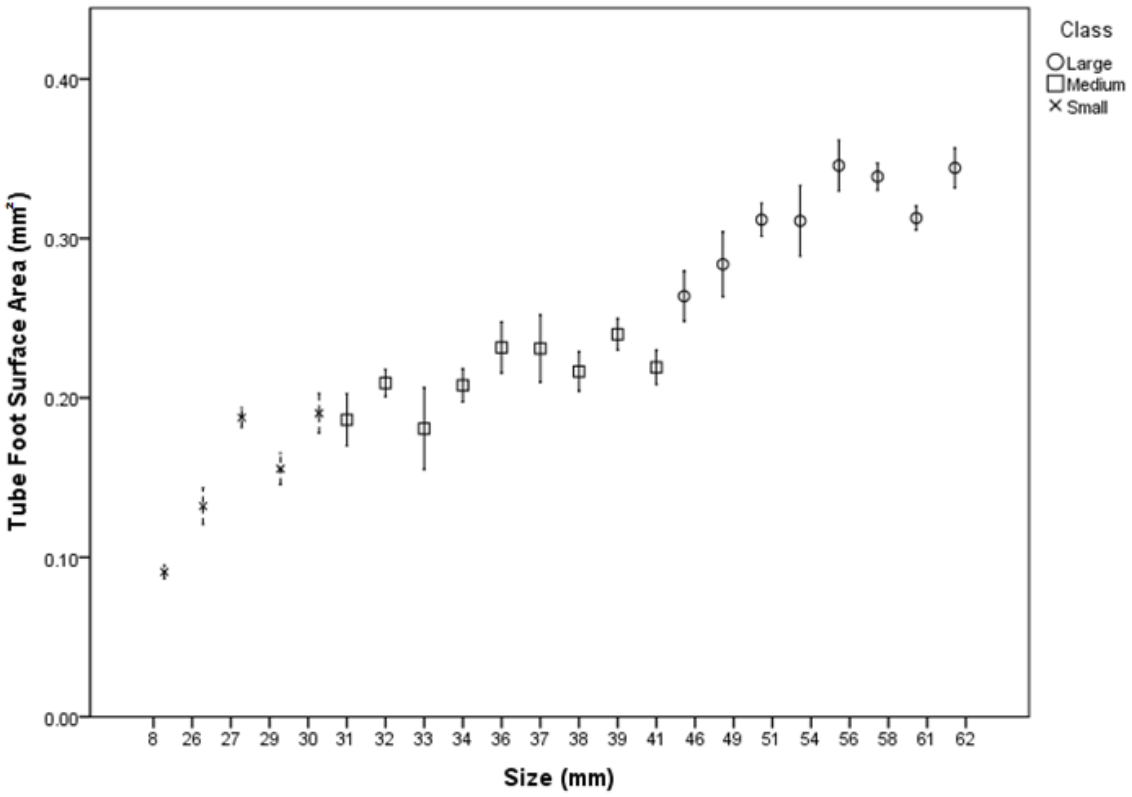

Figure 5: Estimates of podial disc surface area (mm^2) to 1 S.E taken from 10 tube feet footprints for three size classes of *Holopneustes purpurascens* (n=19).

Detachment force

Oral vs Aboral

INSTRON tensile testing of *H. purpurascens* adhering to *Delisea pulchra* revealed a significant difference between oral and aboral sides, with the oral side requiring a greater force to induce detachment over the aboral side (One way ANOVA, $F_{1,128}$=13.073, P<0.01) (Figure 6). A large

amount of variation in detachment force on the aboral side was also observed. In comparison, INSTRON testing revealed no significant difference between force required to detach *H. purpurascens* on either their oral or aboral sides for individuals on *Ecklonia radiata* (One way ANOVA, $F_{1,254}$=2.280; p 0.13) (Figure 7).

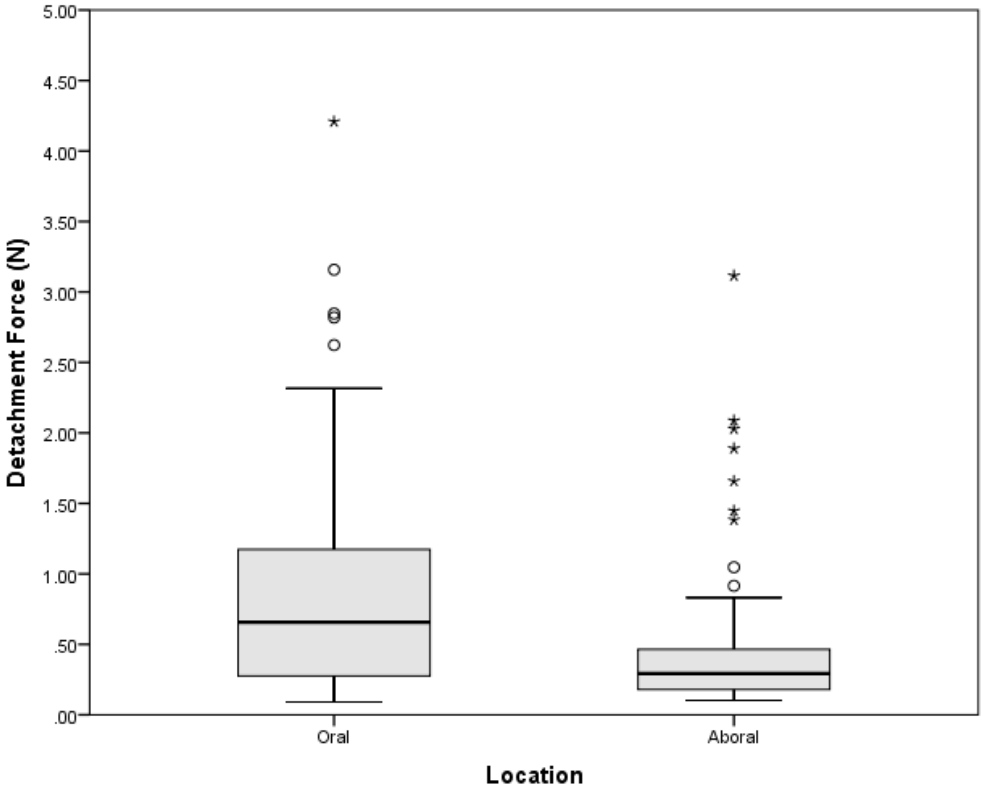

Figure 6: A box plot comparison of the mean detachment force on both the Oral and Aboral sides of *Holopneustes purpurascens* on *Delisea pulchra* (n=65). Outliers marked by small circles and extreme outliers marked as stars.

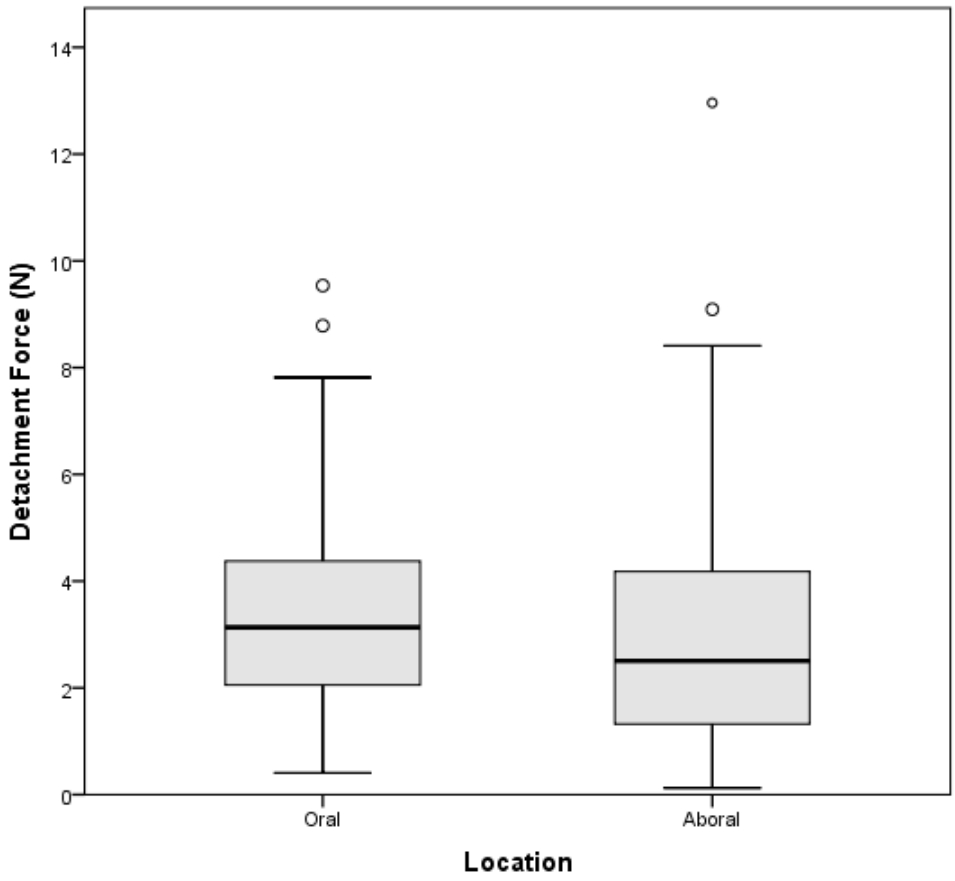

Figure 7: A box plot comparison of the mean detachment force on both the Oral and Aboral sides of *Holopneustes purpurascens* on *Ecklonia radiata* (n=128). Outliers marked by small circles.

Oral - Size Classes

INSTRON mechanical testing revealed that host algae had a significant impact on detachment force (two factor ANOVA, $F_{1,187}$=101.269, P<0.01). Urchins adhering to *E. radiata* required a significantly higher force to induce detachment than the force that was required to detach from *D. pulchra.* A trend of increasing detachment force from small to large size classes was also observed in both *D. pulchra* and *E. radiata,* but was not significant (two factor ANOVA, $F_{2,187}$=1.891, P=0.15). No significant interaction between host algae and size class on detachment force was observed (two factor ANOVA, $F_{2,187}$=0.077, P=0.93) (Figure 8).

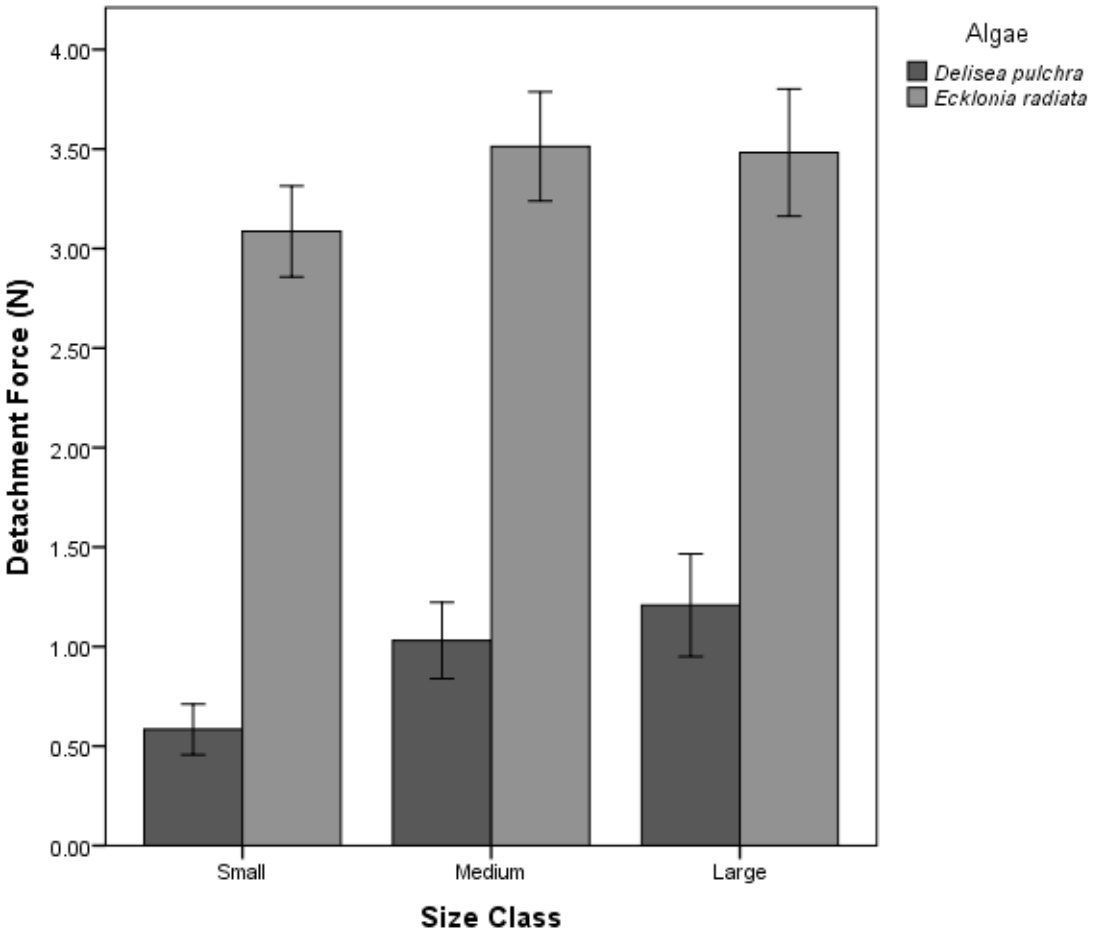

Figure 8: Oral side mean detachment force (±1 S.E) of *Holopneustes purpurascens* adhering to *Delisea pulchra* (n=65) and *Ecklonia radiata* (n=128).

Aboral - Size Classes

Urchins adhering to *E. radiata* required a significantly higher detachment force than those adhering to *D. pulchra* (two way ANOVA, $F_{1,187}$=71.487, P<0.01). In contrast to the oral side, a decreasing trend in detachment force was observed from small to large size classes for urchins in both host algae but was not significant (two way ANOVA, $F_{2,187}$=0.997, P=0.37). There was no significant interaction between host alga and size class (two way ANOVA, $F_{2,187}$=0.060, P=0.94) (Figure 9).

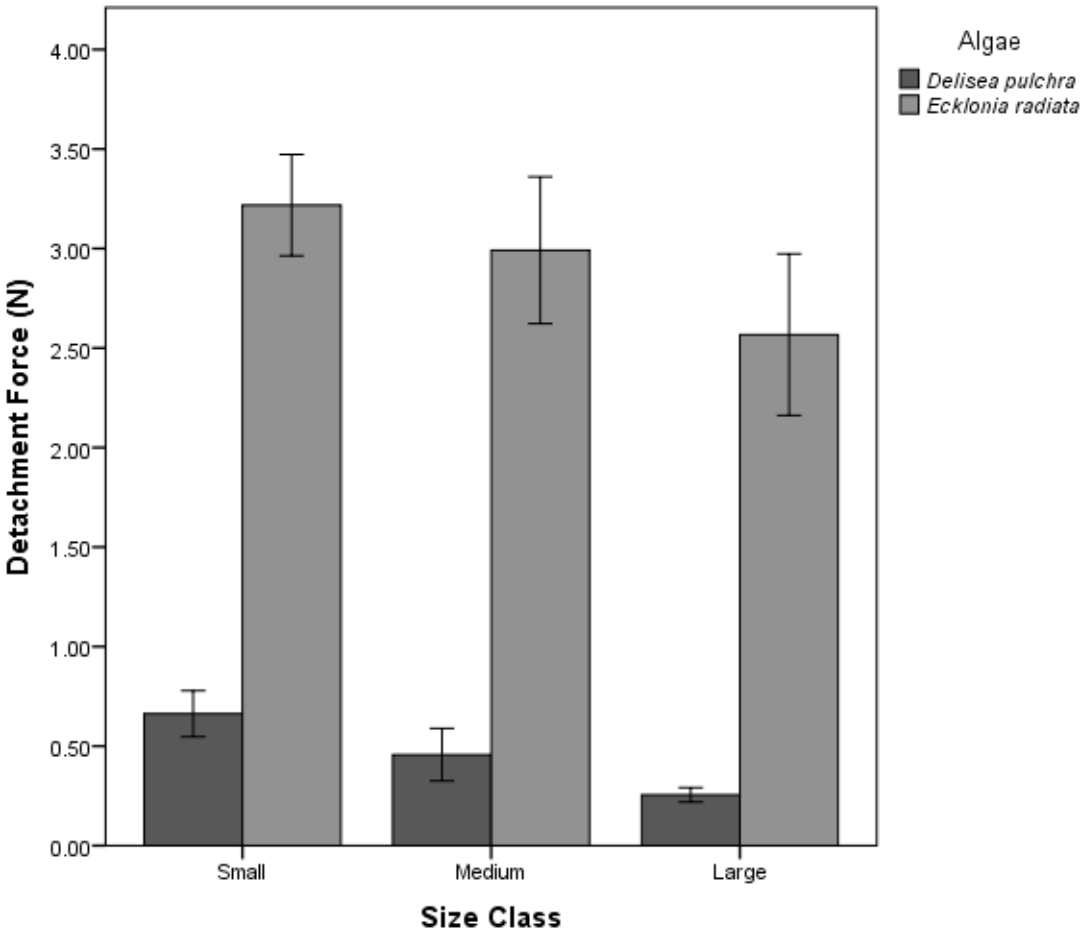

Figure 9: Aboral side mean detachment force (±1 S.E) of *Holopneustes purpurascens* adhering to *Delisea pulchra* (n=65) and *Ecklonia radiata* (n=128).

It should be noted that maximum load did not always represent the load at which *H. purpurascens* became detached from *E. radiata* but rather the load at which tube feet began to disengage from *E. radiata*. Following this, complete detachment often followed, as the number of load bearing tube feet reduced rapidly or were ruptured from *H. purpurascens* test (Connolly, personal observation). Furthermore, due to this and the ecological significance of the oral - feeding - side of *H. purpurascens* (this is the usual site of attachment for this sea urchin); we focused on the oral side henceforth.

Tube feet loss

Tube feet ruptured during detachment force testing indicated that the there was a significant difference in tube feet loss amongst size classes (Welch ANOVA, $F_{2,80.374}$=5.507, P<0.01). Post Hoc Games-Howell test revealed that the small size class lost significantly more tube feet than the medium and large size classes on the oral side (P<0.05) (Figure 10).

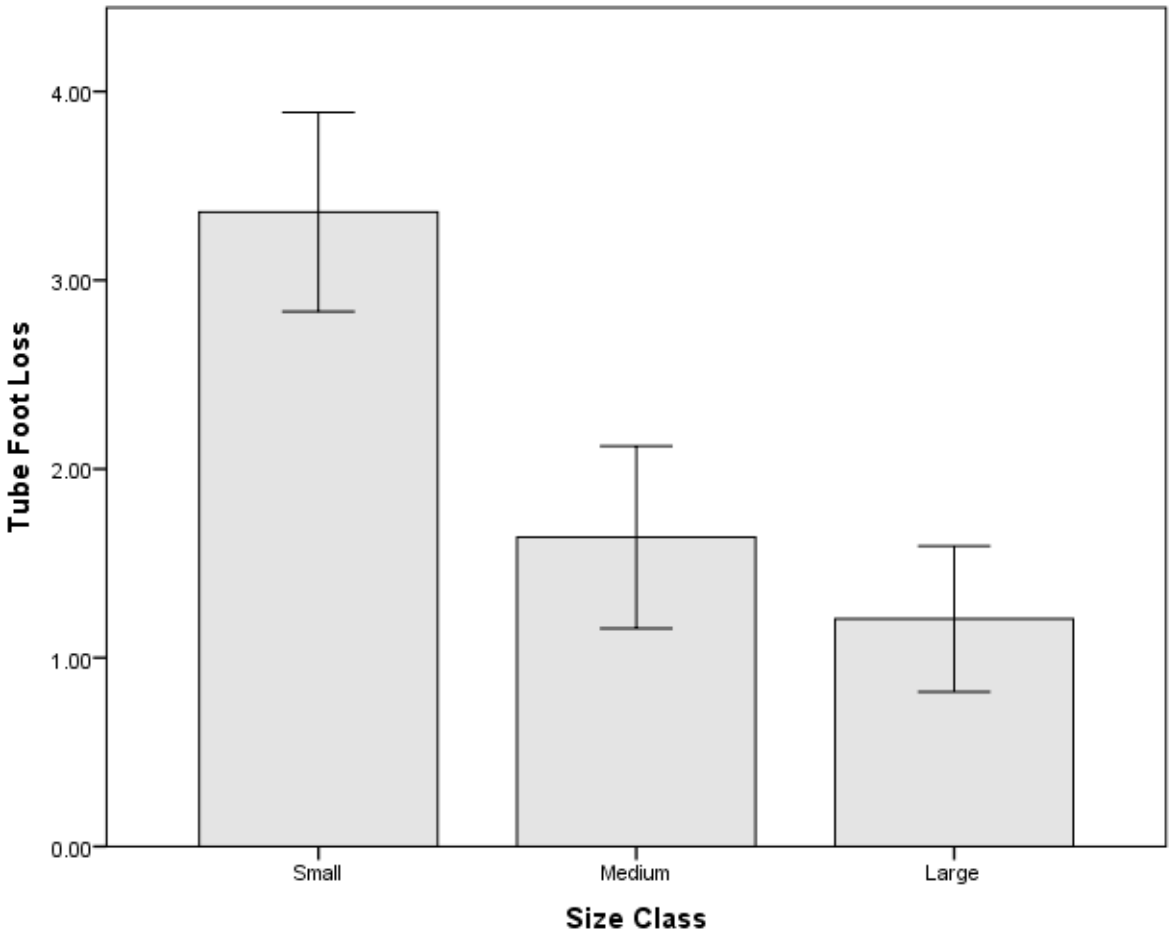

Figure 10: Mean number of tube foot lost during detachment amongst size classes. Taken from the oral side of *Holopneustes purpurascens* (n=128).

Flume

Size Classes

Detachment speed varied significantly between maximum speed and prolonged exposure tests (two factor ANOVA, $F_{1,97}$=64.889, p<0.01). Detachment speed declined across both tests as urchin size class increased (Figure 11). Detachment speed amongst size classes was also found to significantly differ (two factor ANOVA, $F_{2,97}$=47.366, p<0.01), with the subsequent Post Hoc Tukey test revealing the smallest size class had a significantly higher detachment speed than the medium and large size classes (p<0.01) (Figure 11). No significant interaction between experiment and size class was observed (two factor ANOVA, $F_{1,97}$=0.349, P=0.56).

Prolonged exposure in the small size class was not included in the analysis due to a limited number of replicates.

Of the individuals that failed their prolonged exposure test, more than 80% of individuals failed within the first 30 seconds of testing. Observations showed no loss of tube feet during both maximum speed and prolonged exposure testing.

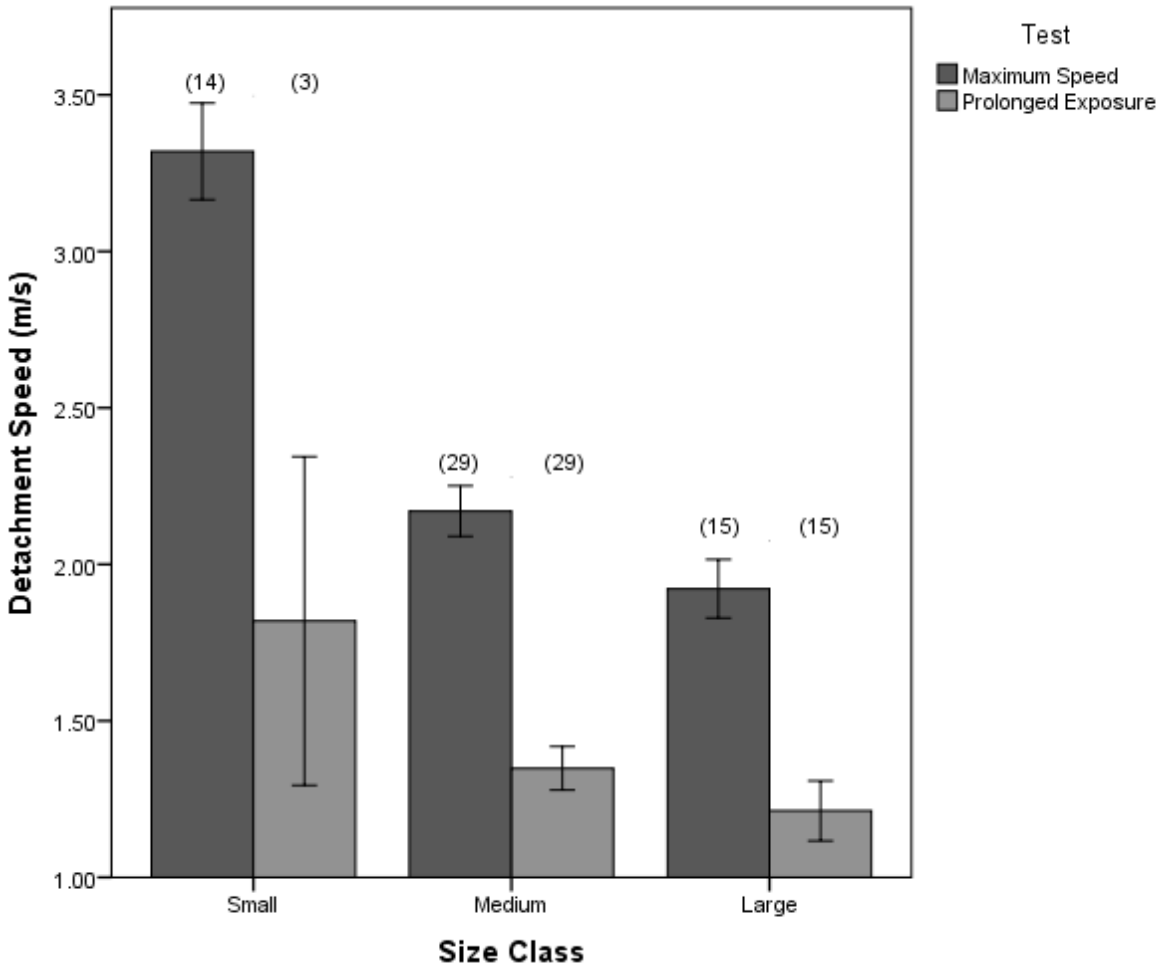

Figure 11: Mean detachment Speed (m/s) for both maximum speed and prolonged exposure (±1 S.E) amongst the small, medium and large size classes of *Holopneustes purpurascens*. Annotations describe the number of replicates in each test under their respective size classes (n=61).

Surface Area

A linear regression between maximum detachment speed and urchin surface area discovered a significant relationship, with detachment speed decreasing linearly with an increase in surface area (R^2=0.482, $F_{3,54}$=16.739, $p<0.01$) (Figure 12). Therefore individuals with a lower surface area could adhere under a greater flow than individuals with a larger surface area, with this trend continuing as surface area increased.

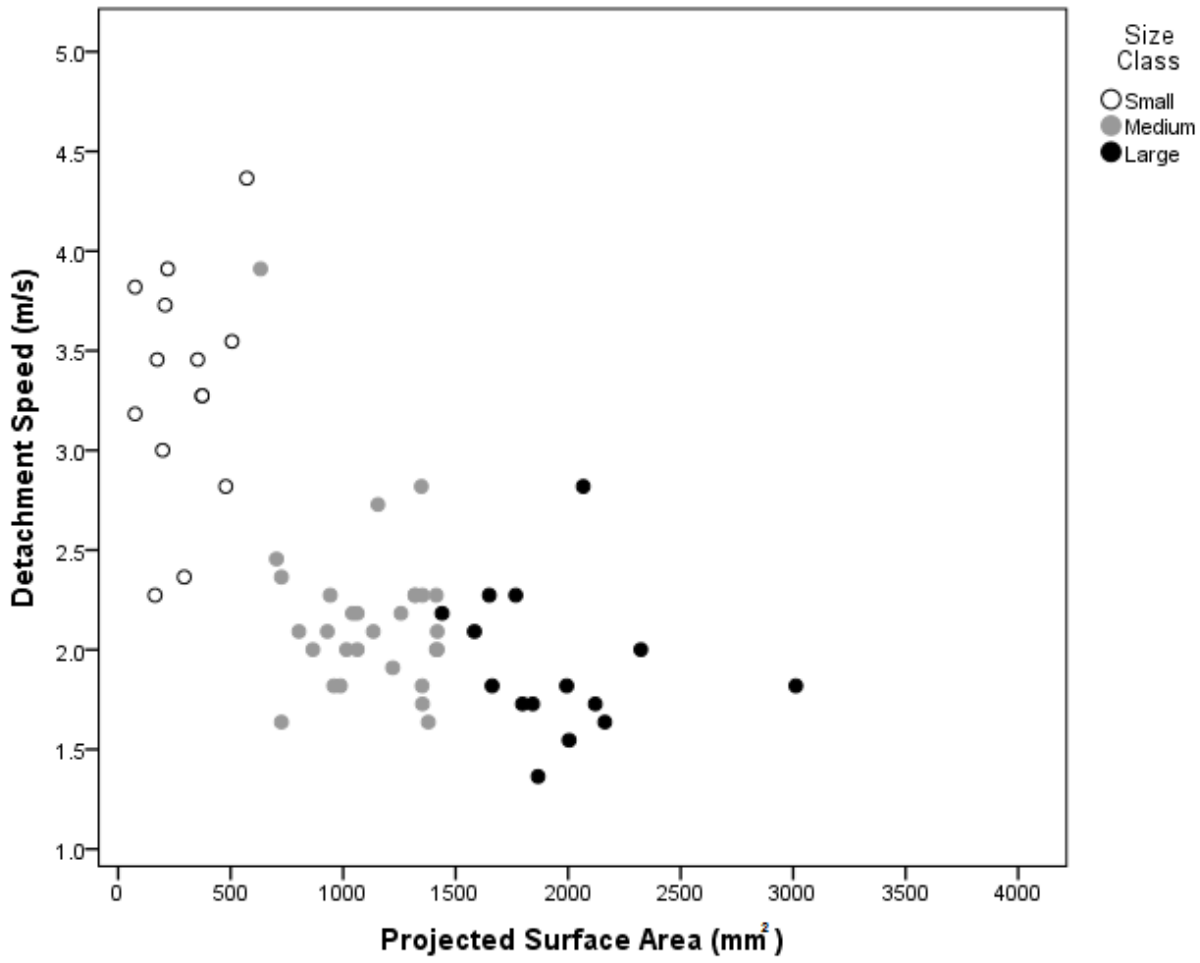

Figure 12: Cubic regression between maximum detachment speed (m/s) and surface area (mm^2) of *Holopneustes purpurascens* categorized under their respective size classes. Equation: Surface Area = 2089.251+567.425(Speed) - 668.252$(Speed)^2$ +104.223$(Speed)^3$.

External morphology of tube feet

Tube feet from all areas of the test were examined and consisted of an extensible cylinder, the stem, which supported a flattened top, the disc (Figure 13A). Tube feet discs were considerably wider than their supporting stem. SEM observations of the tube foot disc revealed two distinct areas: a large central plate separated by a groove from a thin peripheral ring, attached to the stem (Figure 13A, C). Both the central plate and peripheral ring contained cilia (Figure 13B, D). Cilia on the central plate appeared to be uniformly distributed, whilst the central disc depression contained cilia at much higher densities. In contrast, peripheral cilia were

distributed in clusters of 1-5 on the bulges of the ring. Cilia lengths ranged from 1-3µm in the central plate, to 1-2µm in the peripheral ring. Furthermore, the central plate contained a number of pores dotted on its surface, not found on the peripheral ring. The remnants of a glue-like substance was found on the central plate of the disc and may be the remains of temporary gel adhesion (Figure 13G, H).

The internal structure of the tube foot revealed a calcified skeleton composed of two superposed structures – the distal rosette and the proximal frame. Both structures were circularly shaped and situated in a circle around the ambulacral lumen (Figure 14I, J). The rosette was comprised of five large ossicles containing a number of digit-like projections extending to the apical surface of the tube foot disc and corresponds with the bulges located on the peripheral ring (Figure 14K). The frame was devised of several small arc-shaped spicules (Figure 14L).

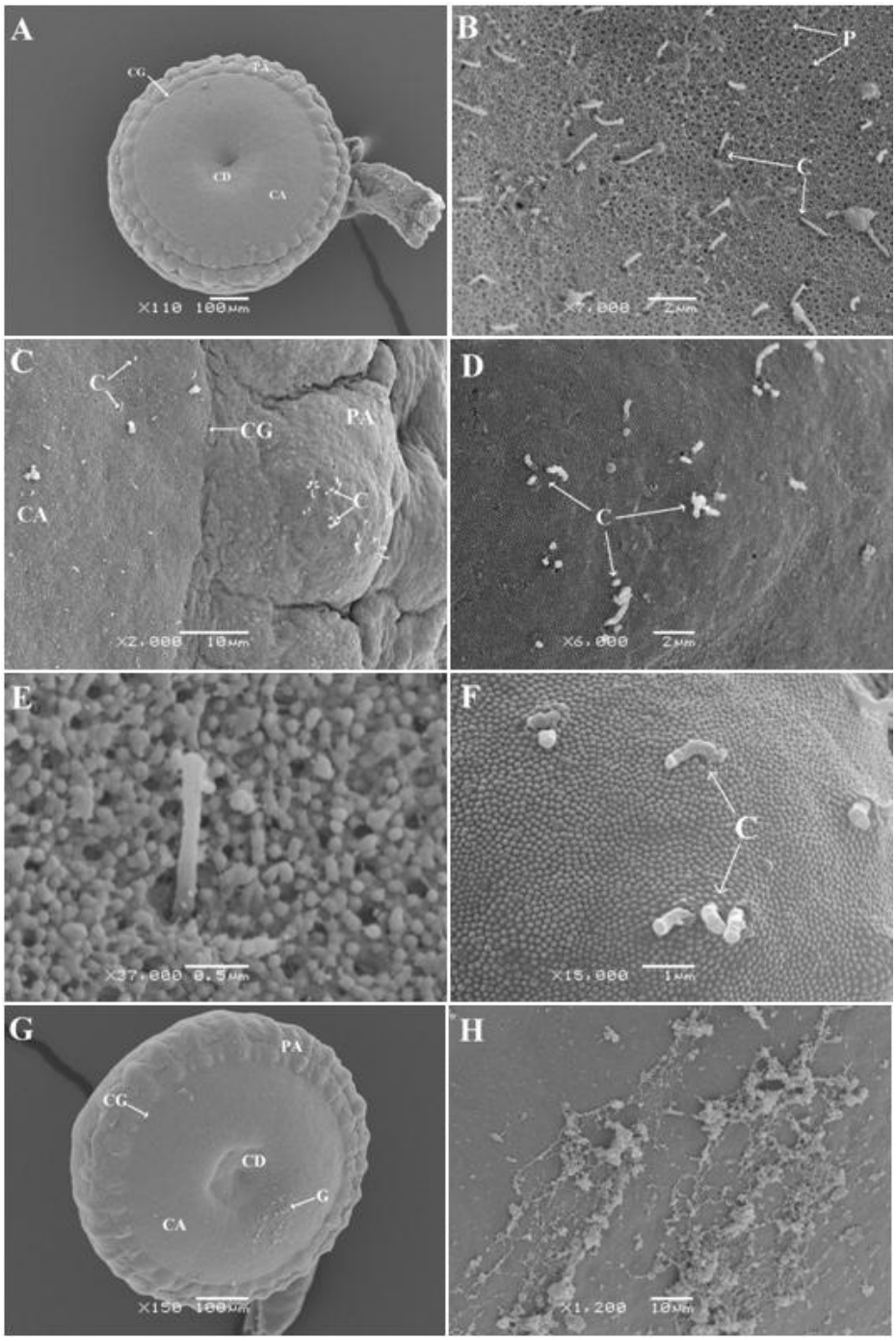

Figure 13: Scanning electron microscopy of the tube foot of *Holopneustes purpurascens* (**A**) General view of a non-attached tube foot (**B**) detail view of the central plate (**C**) circular groove (**D**) peripheral ring (**E**) detailed view of central (**F**) and peripheral hair (**G**) attached tube foot with glue (**H**) detailed view of the glue. Abbreviations: C - cilia, CA - disc central area, CD - disc central depression, CG - circular groove, G - glue, P - pore and PA - disc peripheral area.

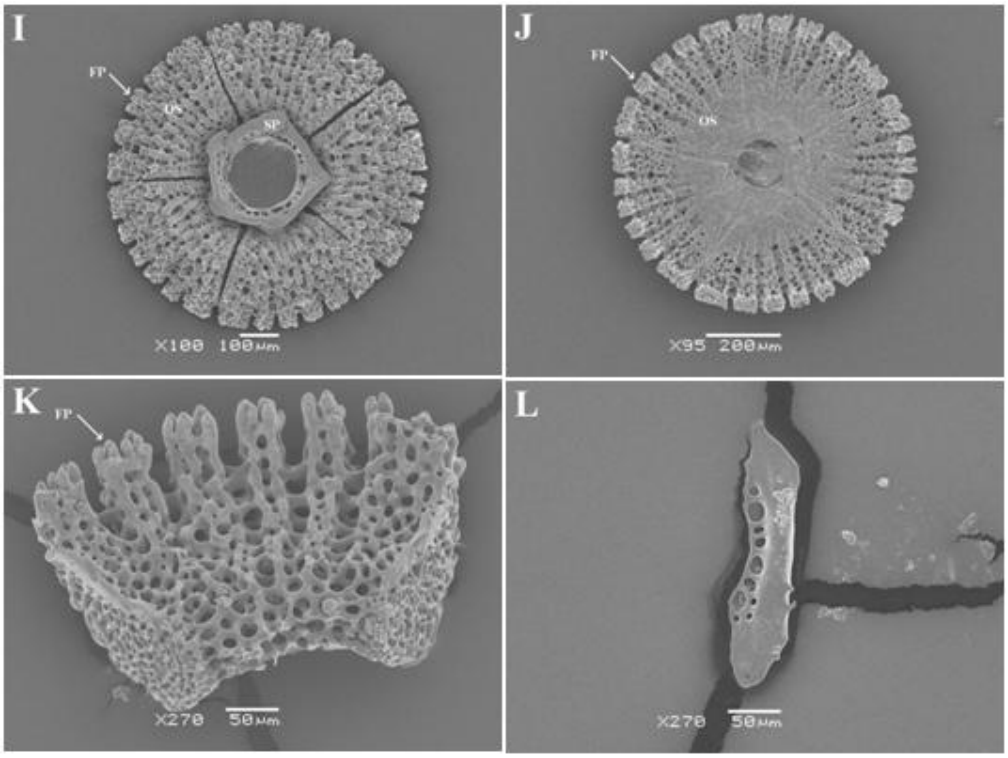

Figure 14**:** Skeletal elements of the tube foot of *Holopneustes purpurascens*. (**I**) Rosette - bottom (**J**) Rosette - top (**K**) detailed view of an ossicle (**L**) detailed view of a spicule. Abbreviations: FP - finger-like projection, OS - ossicle, SP - spicule.

Tube feet histology

The tube foot disc was composed of two layers of differing thicknesses – a deep supporting layer and the distal pad, the layer making contact with the substratum. The supporting structure was devised of a circular plate of connective tissue and comprised of the terminal plate, in contact and continuum of the connective tissue of the stem (Figure 15A, B). The terminal plate sits atop the stem lumen and was much thinner in its centre compared to its margins. The thicker margins held the podial disc skeleton (discussed above) and was responsible for the shape of the disc.

In contrast, the distal pad was comprised of a thick layer of epidermal layer from which the connective tissue protrudes (Figure 15A, B). The distal pad also contained the secretory cells used in adhesion, and is of particular interest due to the number of granules found in their soma (Figure 15C, D). A well defined layer of support cells was found close to the cuticle and

characterised by a large apical neck extending to the discs' surface. These supporting cells also contained a strong structural filament network. Furthermore, between the support cells, an additional network of smaller, darker secretory cells were observed (Figure 15D).

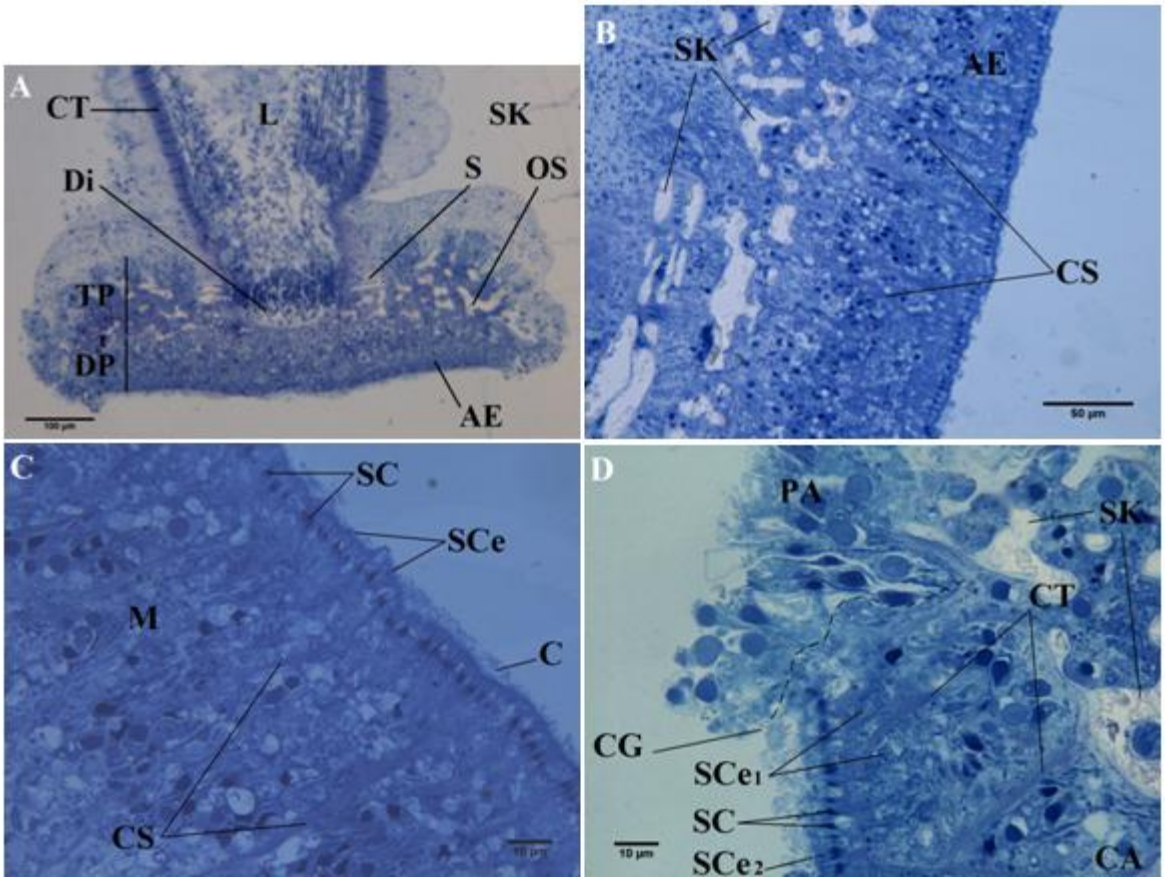

Figure 15: Longitudinal sections through the disc of the tube foot of *Holopneustes purpurascens*. (**A**) General view of the terminal part of the podium (**B**) detail view of the central area of the tube foot disc (**C, D**) the limit between the central area and the peripheral area. Abbreviations: AE - adhesive epidermis, C - cuticle, CA - central area, CG - circular groove, CS - connective tissue protrusion, CT - connective tissue layer, Di - diaphragm, DP - distal pad, L - lumen, M - adhesive epidermis, OS - ossicle, PA - peripheral area, S - spicule, SC - support cell, SCe - secretory cell (SCe1 - type 1, SCe2 - type 2), SK - skeleton and TP - terminal plate.

Discussion

Detachment forces and detachment speeds from size classes of *Holopneustes purpurascens* obtained via INSTRON and flume testing respectively, suggest that adhesion, in conjunction with one or more alternate mechanisms plays a key role in driving the ontogenetic shift of *H. purpurascens*. Our prediction suggested that smaller *H. purpurascens* were unable to colonize the much preferred, but rigid host, *Ecklonia radiata* due to a lack of adhesive strength needed to enmesh themselves within its fronds, and therefore had to settle onto the softer, red algae, *Delisea pulchra*. We defined attachment capacity by the number of tube feet available, disc surface area and footprint attachment quality. Overall we discerned that larger urchins have a greater number of tube feet, a larger disc surface area to apply an adhesive and a greater efficiency of attachment, and therefore would have expected to see this trend reflected in detachment force and detachment speed testing.

Detachment force testing indicated no significant differences between size classes for individuals adhering to *D. pulchra* and *E. radiata*. There was, however, a significant difference in detachment force between urchins adhering *D. pulchra* and those adhering to *E. radiata*. *Holopneustes purpurascens* adhering to *E. radiata* required a detachment force approximately three and a half times of that needed to remove them from *D. pulchra,* suggesting an innate vulnerability to dislodgement on the red alga, and further indicating the unsuitability of *D. pulchra* as a long term host (See Supplementary Figure S2, 3). We suggest that this key finding may be one of the factors driving *H. purpurascens* from *D. pulchra* to *E. radiata*, and may occur through differences in the physical and chemical properties between the host algae. There is also the potential that this difference in detachment force is an artefact of secondary metabolites on *D. pulchra,* which have been shown to initially deter tube feet contact (Williamson 2001). This deterrence may be limiting the number of tube feet adhering to the bed of *D. pulchra,* resulting in a lower force required to induce detachment.

INSTRON detachment force testing also indicated an increasing trend in detachment force as size class increased on both hosts for the oral side, but was reversed on the aboral side. There was no significant difference between the oral and aboral side detachment forces on *E. radiata*

which may be attributed to the opposing increasing and decreasing trends on each side at a similar scale. In contrast the magnitude of difference between the oral and aboral sides on *D. pulchra* was statistically significant. Reduced adhesion on the aboral side in *H. purpurascens* can possibly be attributed to a decreased efficiency of attachment on this location of the urchin's test, with *H. purpurascens* opting for stronger attachment on the oral - feeding - side of the urchin. The aboral side also showed the highest level of variation in footprint attachment in comparison to the ambitus and oral side. Alternatively, this variation could be a result of a lack of tube feet development on the aboral side.

Tube foot loss during INSTRON detachment force testing allowed us to assess the level of structural development within the tube foot amongst different sized urchins. As tube foot disc surface area increased with size, the number of tube feet ruptured at detachment decreased, implying that as tube foot size increases, so does its structural integrity. As an artificial means of detachment testing, the INSTRON experiment does not allow for the complete replication of *H. purpurascens* enmeshment in *E. radiata*. It is probable therefore that smaller urchins would lose more tube feet during detachment from a full enmeshment. Comparatively, the external morphology and ultrastructure of the tube feet of *H. purpurascens* are quite similar to other sea urchin species, with the exception of disc size (Table 1). It has been previously understood that urchins that inhabit high wave energy environments have undergone a higher degree of tube foot development - larger, stickier discs, thicker, stronger stems and a greater number of tube feet involved in adhesion – than those that inhabit lower energy environments (Smith 1978). This may not be the case, as tube foot development does not directly relate to enhanced mechanical properties (Santos & Flammang 2005, Santos & Flammang 2008) (Table 1). Alternatively, a number of other factors including number of tube feet, tube feet arrangement, urchin size and shape have the potential to influence hydrodynamic resistance and, in turn, dictate habitat selection (Santos & Flammang 2005).

The speed at which *H. purpurascens* detached from *E. radiata* decreased with an increase in size class, suggesting that surface area may play a larger role than tube foot development. Urchins that are wider and taller are subjected to increased levels of drag and lift forces and

may be restricted to lower energy environments (Denny et al. 1985, Denny 1999). The effect of this was observed in the relationship between surface area and detachment speed. As surface area increased there was a subsequent decrease in the flow required to induce detachment. Additionally this decline is observed between the small and medium size classes and corresponds to the beginning of the transitional stage of *H. purpurascens* moving from *D. pulchra* to *E. radiata* (Williamson et al. 2004). The decline in detachment speed as size increases may also reveal some insight into the lifespan of *H. purpurascens*. As surface area is directly related to the amount of drag induced, it may indicate a maximum tenable body size living within a hydrodynamic environment. It would also explain the limited number of *H. purpurascens* observed with a test diameter greater than 60mm (Williamson et al. 2004). Due to technical issues with the Flume tank we were unable to exceed 2.25m/s for the prolonged exposure test to determine the final prolonged exposure detachment speed for the small size classed urchins. We can, however, infer that with a prolonged exposure exceeding 2.25m/s, the small size class would again have a significantly higher score than medium and large size classes.

To reduce the hydrodynamic loading of high wave environments many species may inhabit microhabitats such as cracks and crevices. *Holopneustes purpurascens* is no different, living enmeshed amongst *D. pulchra* and *E. radiata,* it benefits from a reduced hydrodynamic loading. Given that the current speeds around Sydney Harbour generally tend to be less than 1 ms^{-1} and rarely exceeding 1.5 ms^{-1}, *H. purpurascens* is adequately equipped to inhabit such a region (Middleton et al. 1996). Furthermore, our flume testing encapsulated *H. purpurascens* adhering to a single unprotected frond of *E. radiata* and may underestimate the true amount of hydrodynamic loading offset from enmeshment amongst an entire host plant. In comparison to other sea urchin species tested *H. purpurascens* mean detachment speeds show that *H. purpurascens* adheres strongly despite the differences in substratum properties (Table 1).

Findings dictate that a number of other potential mechanisms may also be driving this ontogenetic shift and must be explored. Both predation and habitat have been identified as two key drivers of ontogenetic shifts (Werner & Gilliam 1984). These drivers may act either in

synergy or isolation. We explore the likelihood of one or more of these drivers behind the ontogenetic shift of *H. purpurascens*. Predation plays a pivotal role in the distribution and abundance of benthic marine organisms (Gosselin & Qian 1997, Sala et al. 1998, Shears & Babcock 2002). Small individuals are at further risk to this pressure due to the wider range of potential predator sizes and species they are exposed to (Werner and Gilliam 1984, Shears & Babcock 2002). Predation has been shown to drive a number of species into ontogenetic shifts such as the northern abalone *Haliotis kamtschatkana,* who suffers a significant susceptibility to predation until a size threshold is reached (Griffiths & Gosselin 2008). Similarly, the stone crab, *Menippe mercenaria*, appears to be significantly more predated upon during its juvenile stages as opposed to their adult stages (Beck 1995).

Holopneustes purpurascens is particularly susceptible to diurnal predators such as the damselfish, *Parma microlepis*. Observations have shown that predators such as *P. microlepis* are capable of removing 15% of the tube feet and spines of large *H. purpurascens* when transferred to *D. pulchra* beds (Williamson et al. 2004). Loss of only 10% of spines and tube feet occurring at once can onset urchin mortality (Williamson et al. 2004). This inherent vulnerability may shed light on *H. purpurascens* strong diurnal sheltering behaviour, whereby *H. purpurascens* remain tightly enmeshed within their host alga during the day and only expose themselves at night (Williamson et al. 2004). Therefore, it is unlikely that size susceptibility to predation alone is driving *H. purpurascens,* but rather acting in synergy with habitat suitability.

The availability of suitable refuge is paramount to reduce predation, particularly amongst juvenile sea urchins (Sala et al. 1998, Shears & Babcock 2002, Hereu et al. 2005, Feehan et al. 2014). Urchins often shelter within crevices, beneath boulders and amongst algal beds as a means of predator evasion (Sala et al. 1998). Juvenile *Strongylocentrotus droebachiensis* in the presence of kelp holdfasts reduced predation rates by ~20 to 30% when compared to urchins without refuge (Feehan et al. 2014). The presence of *S. droebachiensis* on holdfasts is size distributed, with no adults present on holdfasts (Feehan et al. 2014). The importance of refuge is thought to decrease with size, as urchins become less susceptible to predation once a critical size is reached (Sala et al. 1998, Shears & Babcock 2002, Hereu et al. 2005). This may not be the

case for *H*. *purpurascens*, which has been shown to be vulnerable to predation at all stages in it's life history requiring suitable host protection (Williamson et al. 2004). As a result, *H. purpurascens* may require more complex habitat during their juvenile stage, before moving onto the more suitable long term host, *E. radiata*.

Habitat complexity has been shown to be beneficial to a number of taxa, such as, reef fishes that transition from vegetated near shore environments to deeper, more isolated reef habitats (McCormick 1994; Kimirei et al. 2013). Habitat complexity has also been shown to decrease predation rates amongst the juvenile sea urchin *Paracentrotus lividus*, limiting some post recruitment mortality (Hereu et al. 2005). Organisms may select for these protective environments by settling directly onto them from a larval stage (Ohman et al. 1998). The foliose red algae *D. pulchra* presents a substantially more complex microhabitat than the kelp *E. radiata* for *H. purpurascens*. *Delisea pulchra* may serve as a superior host to smaller *H. purpurascens* which can successfully enmesh themselves in the alga, thus reducing the likelihood of predator detection. Once *H. purpurascens* reaches a particular size threshold, its occupation of *D. pulchra* may be untenable due to its increased chance of visual detection and then, as a result, may shift to *E. radiata.*

Alternatively, *H. purpurascens* may selectively choose to inhabit *D. pulchra* during their early, vulnerable life stage due to the alga's chemical properties. The presence of secondary metabolites within some host algae species is often associated with a reduction in predation in its inhabitants (Hay et al. 1987, Hay & Fenical 1988, Duffy & Hay 1994). These inhabitants benefit from their hosts in a number of ways: protection from predators via sequestration of unpalatable metabolites found on the host, reduced predator detection as a result of a cryptic lifestyle, and the reduction of secondary consumption by herbivores (Duffy & Hay 1994). This relationship has been shown in the amphipod *Ampithoe logimana* which remained unaffected by the chemical defences of its host alga *Dictyota menstrualis* that it preferentially lives and feeds upon (Duffy & Hay 1994). Whilst the abundance of other non-chemically defended species of amphipods declined as a result of an increased abundance of predators, *A. logimana* presence on *D. menstrualis* appeared to be buffered to the increased risk of predation (Duffy &

Hay 1994). *Delisea pulchra* contains a range of non-polar secondary metabolites, furanones, which results in the unpalatability of the host to herbivores (Wright et al. 2004). *Holopneustes purpurascens* that then inhabit *D. pulchra* are in essence protected from marine predators and indirect consumption by herbivores during its early life history (Williamson 2001). Once this early life stage is complete, *H. purpurascens* may be less vulnerable to a broad range of predators and begin to seek out *E. radiata* as a more beneficial long term host.

The availability of habitat can also contribute to size related bottlenecks. *Menippe mercenaria* is limited by the availability of shelter for the successful growth of larger crabs (Beck 1995). Shelter supplemented sites showed an increased moulting and faster reproduction, suggesting that adult crabs in fact suffer from bottlenecks associated with limited refugia, rather than the more susceptible juveniles (Beck 1995). In relation to *H. purpurascens* we believe the availability of *E. radiata* is unlikely to play a role in driving *H. purpurascens* to *D. pulchra* as preliminary host, as the kelp is readily abundant in areas inhabited by *D. pulchra* and other turfing algae.

We conclude that the ontogenetic shift of *H. purpurascens* between *D. pulchra* and *E.* radiata is influenced by the adhesive capacity *H. purpurascens* possesses on both its host alga, in combination with alternate mechanisms such as predation and habitat suitability. To gain a greater insight on the temporary gel adhesion of *H. purpurascens*, future research should consider the examination of the physical and chemical properties influencing adhesion on both *D. pulchra* and *E. radiata*.

Table 1: Comparison of adhesive traits of *Holopneustes purpurascens* and a number of sea urchin species from a range of different habitat types. Data for *Holopneustes purpurascens* was taken from an average of all size classes measured*. Detachment force is represented as *Delisea pulchra*/*Ecklonia radiata*.

Species	**Disc Surface Area (mm^2)**	**Stem diameter (mm)**	**Detachment force (N)**	**Attachment force (N)**	**Mean Detachment force (m/s^{-1})**	**Calculated Detachment force (m/s^{-1})**	**Circular footprints (%)**	**Microhabitat - Wave Energy**	**Reference**
Holopneustes purpurascens	0.24*		0.90/3.35*		1.9*	3.77		Subtidal - Moderate	This study, Williamson et al. 2004
Arbacia lixula	1.07	0.44		3.45	~1.9	5.5	84	Intertidal - High	Santos & Flammang 2007, Santos & Flammang 2005, Tuya et al. 2007
Paracentrotus lividus	0.37	0.31		13.21	~1.0	8.2	37	Intertidal - High	Santos & Flammang 2007, Santos & Flammang 2005, Tuya et al. 2007
Diadem antllarum					~0.65			Subtidal - Low	Tuya et al. 2007
Sphaerechinus granularis	0.62	0.42		33.81		4.6	50	Subtidal - Low	Santos & Flammang 2007, Santos & Flammang 2005
Colobocentrotus atratus	0.8	0.46		16.88		17.5	81	Intertidal - Extreme	Santos & Flammang 2008
Echinometra mathei	0.5	0.39		2.96		7.5	46	Sheltered - Low to High	Santos & Flammang 2008
Heterocentrotus trigonarius	1.0	0.51		14.62		12.5	64	Intertidal to shallow Subtidal - High	Santos & Flammang 2008
Stomopneustes variolaris	0.8	0.51		25.01		10.0	92	Intertidal to Subtidal - High	Santos & Flammang 2008

Acknowledgments

I would like to thank my supervisor Jane Williamson for all of her assistance and guidance throughout the entirety of this project, couldn't have done it without you. I promise to learn the difference between alga and algae some day. Special thanks to Joshua Madin for jumping on board and helping out with both the INSTRON and flume experiments. Thanks to Josh Aldridge and the Sydney Institute of Marine Science for the use of their facility and assistance throughout the flume experiment. I would also like to thank Debra Birch and Nicole Vella for their expertise in microscopy. Thanks to Peter Schlegel for his technical assistance and his prowess in urchin wellbeing. Thanks also to John Connolly for his skilful assistance in building the metal rigs for the INSTRON and Flume experiments. I am also very grateful to all my friends Jennalee Clark, Peter David, Louise Tosetto, Daniel Sokolnikoff, Evan Byrnes, Veronica Shaw and Martin 'microwave' Burnyeat who have helped me with collecting and maintaining my urchin horde. I would like to thank Macquarie University for the opportunity to undertake this project; it has been a huge learning experience. Lastly I would like to give a huge thank you to my mum, dad, family and friends for listening to my weekly urchin updates over the course of this year, you guys are the best.

References

Beck MW (1995) Size-specific shelter limitation in stone crabs: a test of the demographic bottleneck hypothesis. Ecology 76(3):968-980

Bell JE, Bishop MJ, Taylor RB, Williamson JE (2014) Facilitation cascade maintains a kelp community. Mar Eco Prog Ser 501:1-10

Dahlgren CP, Eggleston DB (2000) Ecological processes underlying ontogenetic habitat shifts in a coral reef fish. Ecology 81:2227-2240

Denny M (1999) Are there mechanical limits to size in wave-swept organisms? J Exp Biol 202:3463-3467

Denny MW, Daniel TL, Koehl M (1985) Mechanical limits to size in wave-swept organisms. Ecol Monogr 55:69-102

Dietrich HF, Fontaine AR (1975) A decalcification method for ultrastructure of echinoderm tissues. Stain technol 50(5):351-354

Duffy JE, Hay ME (1994) Herbivore resistance to seaweed chemical defense: the roles of mobility and predation risk. Ecology 75(5): 1304-1319

Feehan CJ, Francis FTY, Scheibling RE (2014) Harbouring the enemy: kelp holdfasts protect juvenile sea urchins from predatory crabs. Mar Ecol Prog Ser 514:149-161

Flammang P (1996) Adhesion in echinoderms. In: Jangoux M & Lawrence JM (eds) Echinoderm studies 5. AA Balkema, Rotterdam, p 1-60

Flammang P, Demeulenaere S, Jangoux M (1994) The role of Podial secretions in adhesion in two species of sea star. Biol Bull 187:35-47

Gosselin LA, Qian PY (1997). Juvenile mortality in benthic marine invertebrates. Mar Ecol Prog Ser 146:265–282

Graham BS, Grubbs D, Holland K, Popp BN (2007) A rapid ontogenetic shift in the diet of juvenile yellowfin tuna from Hawaii. Mar Biol 150:647-658

Griffiths AM, Gosselin LA (2008) Ontogenetic shift in susceptibility to predators in juvenile northern abalone, *Haliototis kamtschatkana*. J Exp Mar Biol Ecol 360:85-93.

Hay ME, Duffy JE, Pfister CA, Fenical W (1987) Chemical defense against different marine herbivores: are amphipods insect equivalents? Ecology 68(6):1567-1580

Hay ME, Fenical W (1988) Marine plant herbivore interactions: the ecology of chemical defense. Annu Rev Ecol Syst 19:111-145

Hereu B, Zabala M, Linares C, Sala E (2005) The effects of predator abundance and habitat structural complexity on survival of juvenile sea urchins. Mar Biol 146:293-299

Kimirei I, Nagelkerken I, Trommelen M, Blankers P, Van Hoytema N, Hoeijmakers D, Huijbers C, Mgaya Y, Rypel A (2013) What drives ontogenetic niche shifts of fishes in coral reef ecosystems? Ecosystems 16:783-796

McCormick MI (1994) Comparison of field methods for measuring surface topography and their associations with a tropical reef assemblage. Mar Ecol Prog Ser 112(1): 87-96.

Middleton JH, Cox D, Tate P (1996) The oceanography of the Sydney region. Mar Pollut Bull 33:124-131

Ohman MC, Munday PL, Jones GP, Caley MJ (1998) Settlement strategies and distribution patterns of coral-reef fishes. J Exp Mar Biol Ecol 225:219-238

Sala E, Boudouresque C, Harmelin-Vivien M (1998) Fishing, trophic cascades, and the structure of algal assemblages: evaluation of an old but untested paradigm. Oikos 82(3):425-439

Santos R, Flammang P (2005) Morphometry and mechanical design of tube foot stems in sea urchins: a comparative study. J Exp Mar Biol Ecol 315:211-223

Santos R, Flammang P (2006) Morphology and tenacity of the tube foot disc of three common European sea urchin species: a comparative study. Biofouling 22:173-186

Santos R, Flammang P (2007) Intra-and interspecific variation of attachment strength in sea urchins. Mar Ecol Prog Ser 332:129-142

Santos R, Flammang P (2008) Estimation of the attachment strength of the shingle sea urchin, *Colobocentrotus atratus*, and comparison with three sympatric echinoids. Mar Biol 154:37-49

Santos R, Gorb S, Jamar V, Flammang P (2005) Adhesion of echinoderm tube feet to rough surfaces. J Exp Biol 208:2555-2567

Shears NT, Babcock RC (2002) Marine reserves demonstrate top-down control of community structure on temperate reefs. Oecologia 132:131-142

Smith AB (1978) A functional classification of the coronal pores of regular echinoids. Palaeontology 21(4):759-789

Smith AM (2006) The biochemistry and mechanics of gastropod adhesive gels. In: Smith AM, Callow JM (eds) Biological adhesives. Springer Berlin Heidelberg, p167-182

Steinberg PD (1995) Interaction between the canopy dwelling echinoid *Holopneustes purpurescens* and its host kelp. Mar Ecol Prog Ser 127:169-181

Swanson RL, Williamson JE, NYS RD, Kumar N, Buckwell MP, Steinberg PD (2004) Induction of settlement of larvae of the Sea Urchin *Holopneustes purpurascens* by histamine from a host alga. Biol Bull 206:161-172

Tuya F, Cisneros-Aguirre J, Ortega-Borges L, Haroun RJ (2007) Bathymetric segregation of sea urchins on reefs of the Canarian Archipelago: role of flow-induced forces. Estuar Coast Shelf S 73(3): 481-488

Vincent SE, Moon BR, Herrel A, Kley NJ (2007) Are ontogenetic shifts in diet linked to shifts in feeding mechanics? Scaling of the feeding apparatus in the banded watersnake *Nerodia fasciata*. J Exp Biol 210:2057-2069

Werner EE, Gilliam JF (1984) The ontogenetic niche and species interactions in size-structured populations. Annu Rev Ecol Syst 15:393-425

Williamson JE (2001) Larval attractants versus adult deterrents: ontogenetic shifts in the response of a sea urchin to host plant chemistry. PhD thesis, University of New South Wales, Sydney, NSW

Williamson JE, Carson DG, de Nys R, Steinberg PD (2004) Demographic consequences of an ontogenetic shift by a sea urchin in response to host plant chemistry. Ecology 85:1355-1371

Wright JT, De Nys R, Steinberg PD (2000) Geographic variation in halogenated furanones from the red alga Delisea pulchra and associated herbivores and epiphytes: Marine chemical ecology. Mar Ecol Prog Ser 207:227-241

Supplementary Material

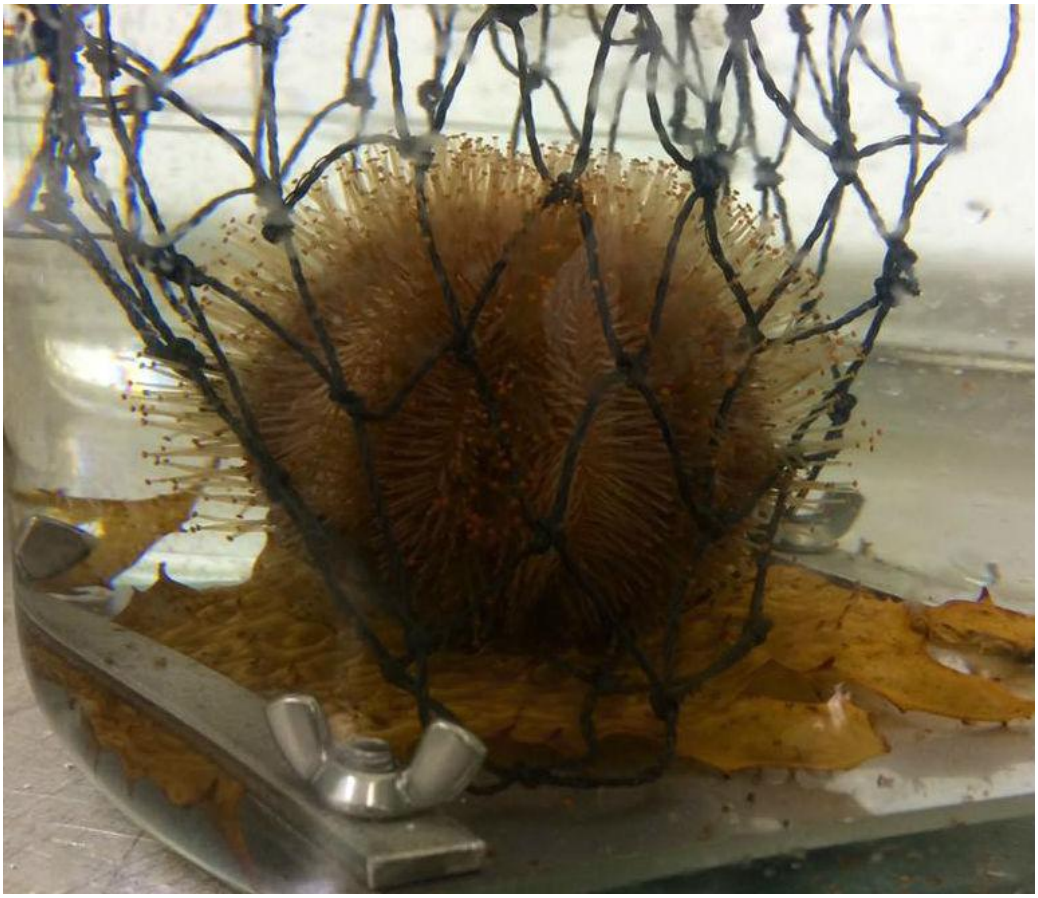

Figure S1: Experiment setup for the INSTRON mechanical testing machine (INSTRON 5542), with *Holopneustes purpurascens* adhering to a frond of the kelp *Ecklonia radiata*, secured to the metal platform.

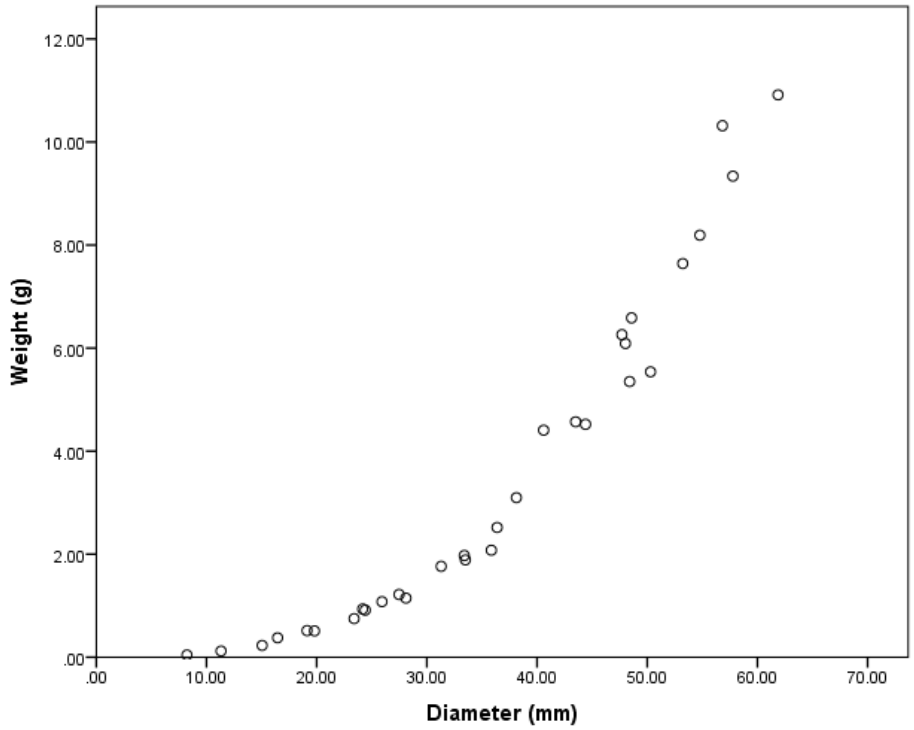

Figure S2: Cubic regression between urchin weight and diameter (R^2=0.985, $F_{3,27}$=572, P<0.01). Equation: Weight=0.640-0.083(diameter) +0.003(diameter)^2 +1.143E-5(diameter)^3.

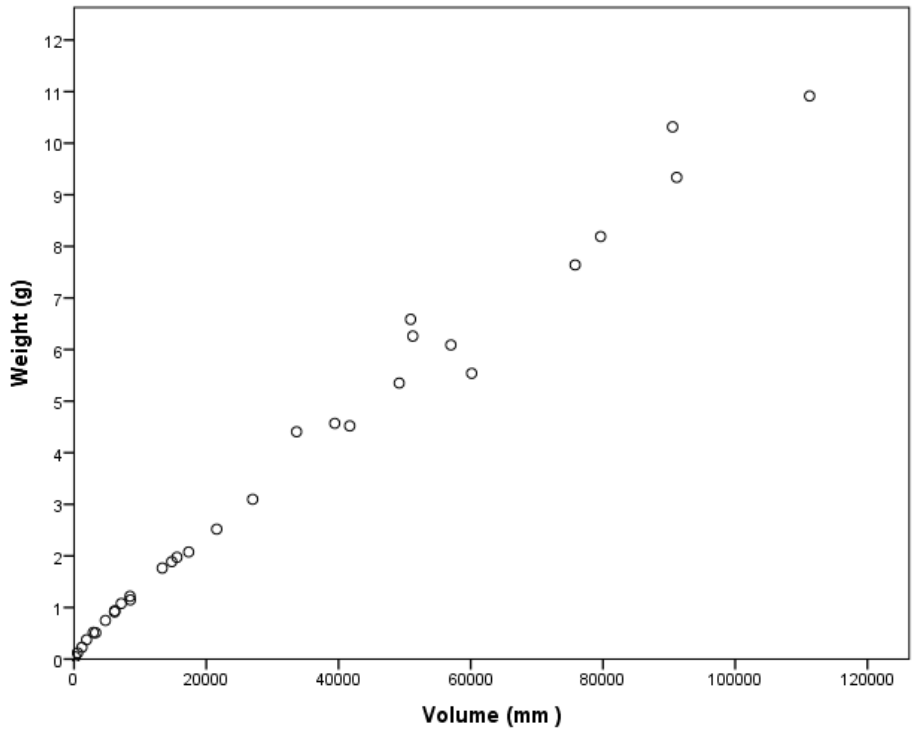

Figure S3:Linear Regression between urchin weight and volume (R^2=0.985, $F_{1,29}$=1941, P<0.01). Equation: Weight = 0.331+0.000x(Volume).